

Evolution of 4*f* electron states in the metal-insulator transition of PrRu₄P₁₂

Kazuaki Iwasa* and Lijie Hao

*Department of Physics, Tohoku University, Sendai 980-8578, Japan*Keitaro Kuwahara, Masahumi Kohgi, Shanta Ranjan Saha,[†] Hitoshi Sugawara,[‡] Yuji Aoki, and Hideyuki Sato
Department of Physics, Tokyo Metropolitan University, Hachioji, Tokyo 192-0397, Japan

Takashi Tayama and Toshiro Sakakibara

Institute for Solid State Physics, University of Tokyo, Kashiwa, Chiba 277-8581, Japan

(Received 15 July 2004; revised manuscript received 8 March 2005; published 6 July 2005)

Magnetic excitations of the filled skutterudite PrRu₄P₁₂ exhibiting a metal-insulator (M-I) transition at $T_{M-I}=63$ K were studied by inelastic neutron scattering experiment. The spectra at temperatures much lower than T_{M-I} are described as well-defined crystal-field excitations. With approaching T_{M-I} , the excitation peaks broaden and shift considerably together with the temperature variation of the carrier number and the atomic displacement in the transition. The 4*f* electron states evolve from the well-localized state in the insulator phase to the strongly hybridized itinerant state by *p-f* mixing near T_{M-I} . The hybridization is responsible for the M-I transition of PrRu₄P₁₂.

DOI: [10.1103/PhysRevB.72.024414](https://doi.org/10.1103/PhysRevB.72.024414)

PACS number(s): 71.70.Ch, 71.30.+h, 78.70.Nx

I. INTRODUCTION

Many rare-earth and actinide compounds have been studied extensively because of their attractive properties such as heavy electrons, unconventional superconductivity, quantum critical behaviors, valence fluctuation, etc. It is commonly accepted that interplay between *f* and conduction electrons is responsible for these properties. The hybridization effect often gives rise to a quasielastic or broad magnetic excitation spectra instead of well-defined crystal-field (CF) excitations.¹ The CF spectral width proportional to temperature in rare-earth systems has been interpreted by so-called Korrington law in which exchange interaction between *f* and conduction electrons is taken into account.² Those of dense Kondo-effect or valence fluctuation systems often show $T^{1/2}$ -behavior. It was theoretically studied based on the degenerate Anderson model.^{3,4} To understand the complex magnetic structures of Ce-monopnictides, the effect of *p-f* mixing between 4*f* electrons and *p* holes of the pnictogens on the CF levels was discussed.⁵ It succeeded in explaining the anomalously small CF split between a ground state and an excited state.

Recently, filled skutterudite RT_4X_{12} (R =lanthanide and actinide elements, T =transition metal, X =pnictogen) has been found to show various physical properties involving *f* electrons.⁶ In their crystal structure with the space group $Im\bar{3}$ (T_h^5), X atoms form corner shared octahedra. T and R ions are located inside and between the octahedra, respectively. Since R ions are surrounded by 12 X atoms forming an icosahedron, it is suggested that the various properties originate from the *p-f* mixing.⁷ Among them, PrRu₄P₁₂ exhibits a metal-insulator (M-I) transition at $T_{M-I}=63$ K.⁸ Electron and x-ray diffraction studies elucidated a superlattice characterized by the wave vector $\mathbf{q}_0=(1,0,0)$ with $Pm\bar{3}$ (T_h^1) below T_{M-I} .⁹⁻¹¹ The band structure study proposed that the Fermi surfaces perpendicular to the $[1,0,0]$ axes cross half way between Γ and X points to form a cubiclike shape.¹² Thus, this

phase transition is suggested to be a charge-density-wave (CDW) formation owing to a three-dimensional Fermi-surface nesting by \mathbf{q}_0 . No anomaly of magnetic susceptibility was observed at T_{M-I} (Ref. 8) and the CF ground state was suggested to be nonmagnetic from the specific heat measurement.¹³ However, an isotropic magnetic moment of about $1\mu_B/\text{Pr}$ is induced under a magnetic field less than 1 T at lower temperature, as presented in this paper. There has been no trace of magnetic ordering. The electrical resistivity turns up below T_{M-I} and shows shoulderlike anomaly around 40 K. From these facts, it is natural to expect a contribution of 4*f* electrons to the M-I transition. Since the magnetic excitation spectrum by 4*f* electron CF levels reflect the carrier state as mentioned above, the 4*f* electron role in the M-I transition of PrRu₄P₁₂ can be investigated by the magnetic excitation measurement.

To understand the 4*f* electron state and the anomalous magnetic state in the M-I transition of PrRu₄P₁₂, we carried out an inelastic neutron scattering measurement. Clear sharp CF excitations of Pr³⁺ 4*f*² electrons are observed at temperatures much lower than T_{M-I} . It is remarkable that, with increasing carrier number by elevating temperature, the CF excitation peaks shift and broaden drastically. We will show that PrRu₄P₁₂ undergoes the M-I transition mediated by strongly hybridized state between 4*f* electrons and carriers.

II. EXPERIMENTAL

A polycrystalline sample was prepared by the Sn-flux method, whose quality is similar to that used in the transport study.¹⁴ The inelastic neutron scattering experiments were performed at the time-of-flight spectrometers LAM-D (thermal neutron) and LAM-40 (cold neutron) installed in the pulsed neutron facility KENS in KEK, Japan. Scattered neutrons with the energy of 4.59 meV selected by pseudo-mirror-type pyrolytic graphite crystal analyzers were

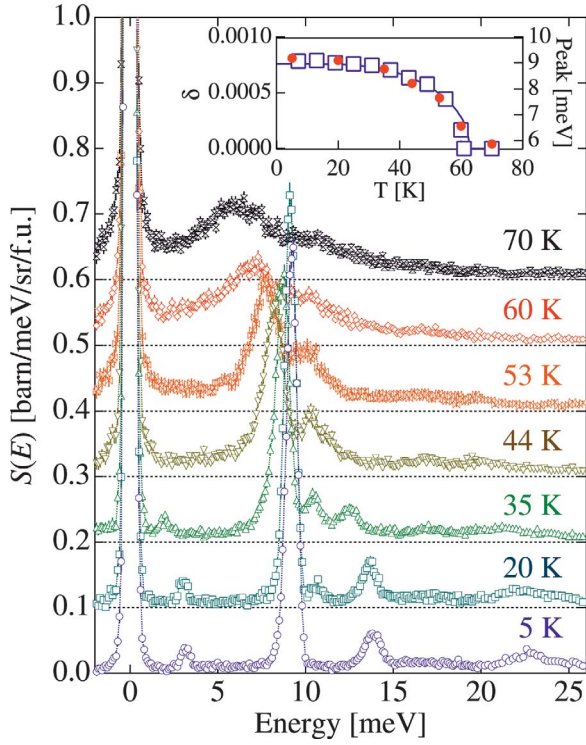


FIG. 1. (Color) The symbols represent $S(E)$ of $\text{PrRu}_4\text{P}_{12}$ measured at LAM-D. Origins of vertical axes of each temperature data are shifted by 0.1. In an inset, open squares depict temperature dependence of the Ru-ion displacement δ in units of atomic coordinate determined in the x-ray diffraction study (Ref. 11), a solid line is the BCS gap function fitted to δ , and filled circles are the position of the highest inelastic neutron scattering peak.

counted by four or seven detectors at LAM-D and LAM-40, respectively. Sample temperatures were controlled between 5 and 70 K by a cryostat with continuous flow of liquid He.

III. RESULTS AND DISCUSSION

Figure 1 represents the temperature dependence of the response functions $S(E) = (1/N)(k_f/k_i)^{-1}(d^2\sigma/d\Omega dE_f)$ obtained at LAM-D. These are evaluated by correcting absorption, subtracting the background estimated from the measurement without the sample, and transforming to absolute cross sections by incoherent scattering intensity of vanadium.

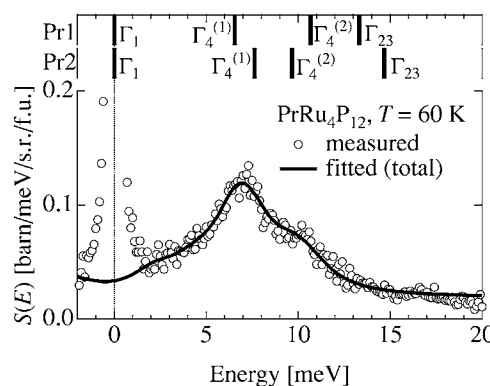
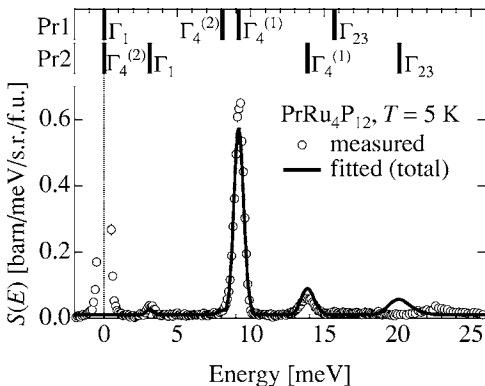


FIG. 2. The circles are measured spectra at 5 K (left part) and at 60 K (right part). The lines are the fitted results by the model of two CF level schemes. The vertical bars represent CF energies at Pr1 and Pr2 measured from each ground state.

At 5 K, clear peaks are seen at 3.2, 9.3, 13.9, and 22.7 meV. Although the width of the last peak is broader than the instrumental resolution in contrast to the other peaks having almost resolution-limited widths, they are presumably attributed to CF excitations, since the scattering-angle dependence of intensity is consistent with that of magnetic form factor of Pr^{3+} . It is noticeable that, with increasing temperature, the peaks shift to the lower-energy side and become very broad. Such drastic behavior will be discussed based on the strong electron hybridization. Open squares in the inset of Fig. 1 depict temperature dependence of Ru-ion displacement δ determined by the x-ray diffraction study, where the Ru ions are located at $(1/4 + \delta, 1/4 + \delta, 1/4 + \delta)$ and the equivalent positions.^{9–11} The maximum-intensity position of inelastic spectra indicated by circles as well as δ corresponding to the order parameter obey the BCS-type gap function for the CDW state shown by a solid line. Then it is natural to consider the CF levels variation coupling strongly with the carrier state and the structural change.

Because of the superlattice structure below T_{M-I} , local environments around the Pr ions at the unit-cell origin and at the body center are different. Therefore, there should be two level schemes for each Pr-ion sites (Pr1 and Pr2) below T_{M-I} . The CF Hamiltonian for 4f electrons in both of $\text{Im}\bar{3}$ and $\text{Pm}\bar{3}$ structures is represented as

$$\mathcal{H}_{\text{CF}} = A_4(O_4^0 + 5O_4^4) + A_6^c(O_6^0 - 21O_6^4) + A_6^t(O_6^2 - O_6^6), \quad (1)$$

where O_m^n expresses a Stevens' operator equivalent.¹⁵ The last term of A_6^t is caused by the lack of the point symmetry C_4 in T_h . The 4f² electron state of Pr^{3+} split to four levels; a singlet Γ_1 , a nonmagnetic non-Kramers doublet Γ_{23} , and triplets $\Gamma_4^{(1)}$ and $\Gamma_4^{(2)}$. We carried out a least-squares fitting procedure of calculated CF excitation spectra in the full measured energy range to the data of $S(E)$ at 5 K. We took free parameters of the CF coefficients in Eq. (1), a scale factor for a ratio of calculated cross section to the experimental result, and a constant background to approximate the phonon contribution, which is very small compared with the CF excitation peaks. The peak widths are assumed to be equal to the instrumental resolution. The result shown by solid lines in the upper figure of Fig. 2 reproduces well the experimental data shown by circles, except the broad peak observed at 22.7 meV.

TABLE I. The CF coefficients and scale factors obtained from the analysis of $S(E)$.

Parameter	5 K	20 K	35 K	44 K	53 K	60 K	70 K
$A_4(\text{Pr1})$ (mK)	-6.816	-5.571	-16.69	-14.10	-12.90	-17.17	-15.06
$A_6^c(\text{Pr1})$ (mK)	0.9505	0.952	0.860	0.879	0.844	0.715	0.729
$A_6^t(\text{Pr1})$ (mK)	0.46	0.41	2.01	2.56	2.36	5.69	7.31
$A_4(\text{Pr2})$ (mK)	41.2	42.7	22.25	17.45	13.83	-11.50	-15.06
$A_6^c(\text{Pr2})$ (mK)	1.41	1.45	0.944	0.916	0.794	0.847	0.729
$A_6^t(\text{Pr2})$ (mK)	10.0	8.07	7.50	7.43	8.68	3.09	7.31
Scale	0.940	1.001	0.850	0.888	0.986	1.067	1.227

The best fit CF coefficients are shown in Table I. It is characteristic that, in the lower temperature region, the ground state of Pr1 is nonmagnetic Γ_1 and the first excited state magnetic $\Gamma_4^{(2)}$, and vice versa for Pr2. In order to check the validity of the obtained CF scheme, we calculated magnetization based on the CF coefficients at 5 K. As shown in Fig. 3, the resultant isotropic magnetization dominated by the $\Gamma_4^{(2)}$ ground state of Pr2 agrees quite well with the experimental data at 60 mK.

The discrepancy between the observation and the calculation at low fields can be dissolved by taking into account a split of the $\Gamma_4^{(2)}$ expected from the observed Schottky peak of specific heat at 0.3 K, although the origin of the split is unknown. Because the nearest-neighbor Pr ions (Pr1) of Pr2 are nonmagnetic, no magnetic ordering is naturally expected. The specific heat value of $0.51 \text{ J K}^{-1} \text{ mol}^{-1}$ at 9 K evaluated from the CF parameters at 5 K, corresponding to an excitation from $\Gamma_4^{(2)}$ to Γ_1 of Pr2, is close to the observed value of $0.6 \text{ J mol}^{-1} \text{ K}^{-1}$.¹³ Such quantitative agreement with the magnetization and the specific heat supports the present assignment of the CF levels.

For analyzing the data at higher temperatures, the CF peaks are assumed to be expressed by Lorentzians with a finite width adjusted in the fitting procedure involving convolution of the instrumental resolution. Since the two Pr-ion sites are equivalent above T_{M-I} , we analyzed the data at 70 K under constraint of the same CF parameters for Pr1 and Pr2.

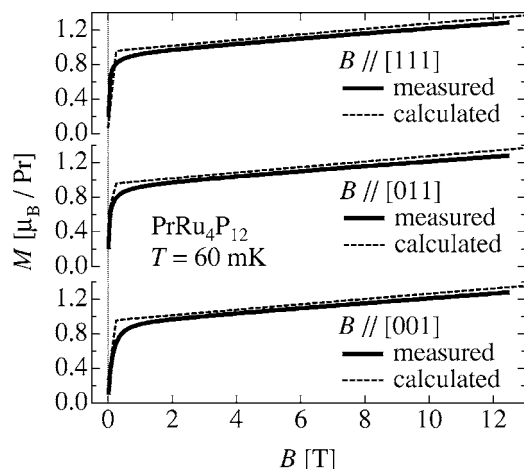


FIG. 3. The magnetizations measured at 60 mK (solid lines) and those calculated from the CF parameters at 5 K (dotted lines).

As shown in the lower part of Fig. 2, the fitted curve agrees well with the experimental result at 60 K. The resultant parameters are listed in Table I. The values of CF Hamiltonian coefficients do not show a smooth dependence on temperature. This is due to the following reasons. The cross section of the excitation from the ground state Γ_1 to $\Gamma_4^{(2)}$ at 8.14 meV of Pr1 at 5 K is about 3% of that from Γ_1 to $\Gamma_4^{(1)}$ at 9.27 meV, which were resolved only in the higher-resolution measurement at LAM-40. The cross section of the excitation from $\Gamma_4^{(2)}$ to Γ_1 at Pr2 is also small. These smaller peaks are hidden at the high temperature region because of the spectral broadening. Thus, the determination of the small-peak position and intensity shown in Fig. 1 contains uncertainty. However, the overall spectra are well fitted and the scale factors are almost one as tabulated in Table I. We compared also the temperature of bulk magnetic susceptibility with that of the CF schemes determined in the present neutron scattering study. As seen in Fig. 4, the magnetic susceptibility measured under magnetic field of 0.1 T applied along the $[0, 0, 1]$ axis (a solid line) agrees quite well with that calculated from the presently determined CF Hamiltonian parameters as well as the Zeeman term (open squares). Thus, the present analysis succeeds in reproducing the experimentally determined cross sections quantitatively.¹⁶

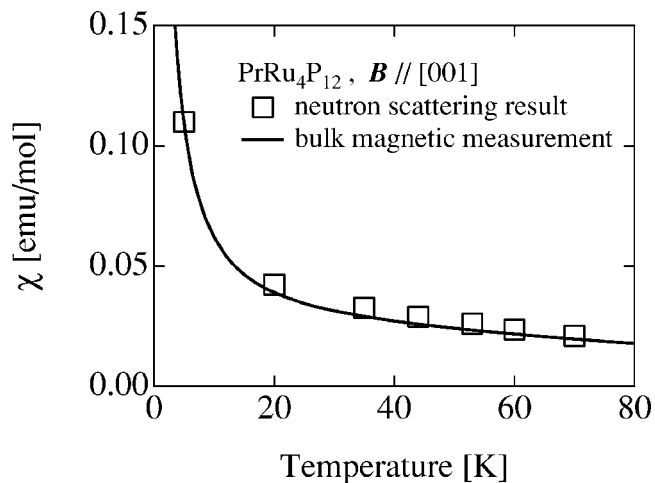


FIG. 4. The solid line represents measured bulk magnetic susceptibility under magnetic field applied along the $[0, 0, 1]$ axis, and the open squares the calculated one based on the CF parameters determined in the present neutron scattering experiments.

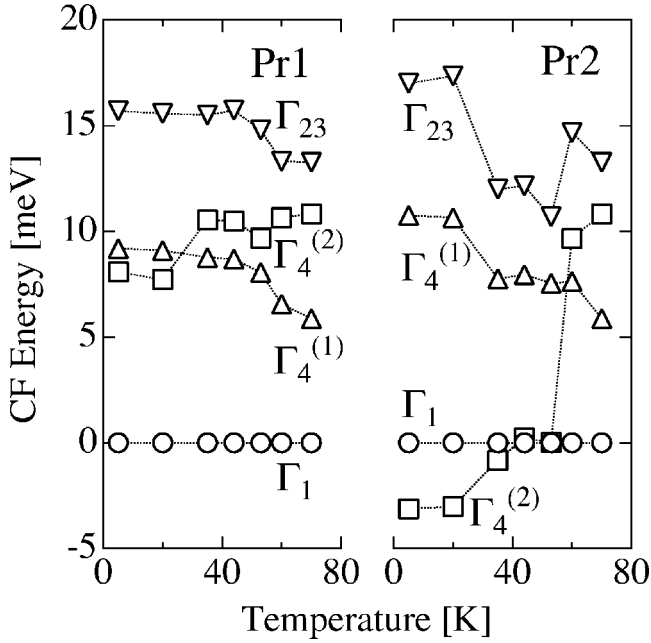


FIG. 5. The CF level schemes of Pr1 and Pr2 as differences from Γ_1 .

Figure 5 shows the resultant temperature variation of the level schemes of Pr1 and Pr2, in which the zero energy is at the Γ_1 level.

The nonmagnetic ground state Γ_1 of both Pr1 and Pr2 around T_{M-I} is consistent with the suggestion from magnetic susceptibility and specific heat data.^{8,13} The ground state of Pr2 switches to $\Gamma_4^{(2)}$ below about 40 K. This switch may give rise to the plateau of electrical resistivity at around this temperature.⁸ As depicted by symbols in Fig. 6(a), the intrinsic half-width at half-maximum (HWHM) varies from ~ 0 at 5 K to 1.73 meV at 70 K. This unusual CF evolution evidences a strong interaction of 4*f* electrons with carriers.

The observed peak broadening will be analyzed by the following form of the HWHM $\gamma(T)$ up to $T \cong 6\Delta_{CF}$, where Δ_{CF} is the CF split energy, expressed as

$$\gamma(T) = \gamma(0) + 4\pi[J_{ex}(g_J - 1)N(E_F)]^2 k_B T, \quad (2)$$

where J_{ex} denotes an exchange integral between 4*f* and conduction electrons and $N(E_F)$ the density of states at the Fermi level.² In contrast to conventional metals showing *T*-linear behavior of $\gamma(T)$ due to temperature-independent $N(E_F)$, the broadening of CF peaks in PrRu₄P₁₂ is strongly nonlinear against *T* as depicted in Fig. 6(a). This phenomenon can be ascribed to the variation of electronic state of PrRu₄P₁₂ in the M-I transition. We analyze the data based on Eq. (2) by simply assuming that the $N(E_F)$ is proportional to the carrier number $n(T)$. It is presumed to be expressed as

$$n(T) = n_0 e^{-\Delta_g(T)/k_B T}, \quad (3)$$

where $\Delta_g(T)$ is an activation energy following the BCS gap function reproducing the atomic displacement below T_{M-I} as shown in the inset of Fig. 1. $\Delta_g(0) = 37$ K is evaluated from the electrical resistivity.⁸ Calculating $\gamma(T)$ by substitut-

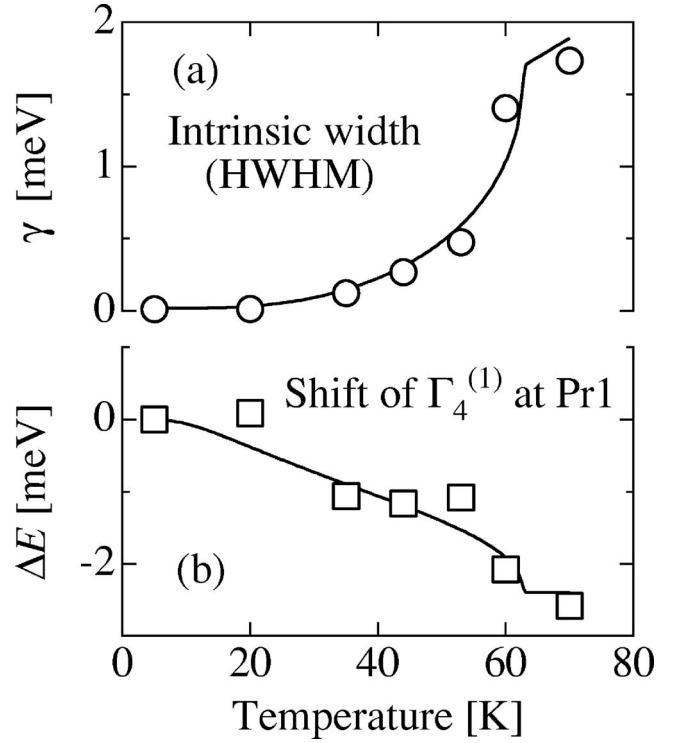


FIG. 6. (a) The circles are the HWHM of CF peaks and a line calculated one based on Eqs. (2) and (3). (b) The squares are the shift of eigenenergy of $\Gamma_4^{(1)}$ at Pr1 and line based on Eq. (3).

ing $n(T)$ for $N(E_F)$ and by putting arbitrary values of $\gamma(0) = 0.016$ meV and $J_{ex}n_0 = 0.23$ reproduces the experimental HWHM well, as shown by a line in Fig. 6(a). The success of this simple analysis supports that the hybridization effect becomes significant with increasing temperature near T_{M-I} .

The shift of CF excitation peaks is also explained by the carrier-state variation in the M-I transition. The *p-f* mixing forces the valence band level to be raised and the mixed CF level to be lowered.⁵ The CF energy shift is proportional to the number of holes in the valence band. In the case of PrRu₄P₁₂, the holes in the 49th band are thought to be responsible for the *p-f* mixing.¹² As it is reduced below T_{M-I} , the mixed CF level energy is expected to increase. In addition, to keep the center of gravity of the CF energy, even the CF levels with less mixing also shift. In Fig. 6(b), the experimentally determined shift of eigenenergy of $\Gamma_4^{(1)}$ at Pr1 is shown as a typical example, together with a line of $-n(T)$ in Eq. (3) with an arbitrary value of $n_0 = 2.4$. Their temperature variations are similar to each other, so that the strong hybridization between *f* electron orbit and *p* electron holes at the high-temperature region is again supported.

IV. SUMMARY

It is concluded that the M-I transition of PrRu₄P₁₂ is a new type of CDW transition mediated by the strong hybrid-

ization between $4f$ electron and carrier states. Above T_{M-1} , the instability of the p hole band due to the three dimensionally perfect nesting is enhanced by the high density of state at the Fermi level owing to the hybridization effect, as evidenced by the present work. It gives rise to the CDW transition resulting in the lowering of the band energy by the gap formation and losing the hybridization with $4f$ electron state. This scenario can explain the observed evolution of the $4f$ electron state through the transition, and also explain the reason why $\text{LaRu}_4\text{P}_{12}$ without the $4f$ electron does not undergo a CDW transition in spite of similar nesting conditions as that of $\text{PrRu}_4\text{P}_{12}$.¹⁷

ACKNOWLEDGMENTS

The authors acknowledge greatly Professor H. Harima and Dr. K. Matsuhira for their fruitful discussions and the neutron-scattering instrument group LAM at KEK for the experimental assistance. This study is partially supported by the Grants-in-Aid for Scientific Research from Ministry of Education, Culture, Sports, Science and Technology, Japan [Young Scientists (B) (No. 15740219) and Scientific Research Priority Area “Skutterudite” (No. 15072206)]. One of the author (L.H.) is supported by the JSPS Postdoctoral Fellowship for Foreign Researchers.

*Electronic address: iwasa@iiyo.phys.tohoku.ac.jp

†Present address: Department of Physics and Astronomy, Faculty of Science McMaster University, Canada.

‡Present address: Department of Mathematical and Natural Sciences, Faculty of Integrated Arts and Sciences, The University of Tokushima, Tokushima 770-8502, Japan.

¹E. Holland-Moritz and G. H. Lander *Handbook on the Physics and Chemistry of the Rare Earths Vol. 19* (Elsevier Science B. V., Amsterdam, 1994), p. 1.

²K. W. Becker *et al.*, *Z. Phys. B* **28**, 9 (1977).

³Y. Kuramoto and E. Müller-Hartmann, *J. Magn. Magn. Mater.* **52**, 122 (1985).

⁴D. L. Cox *et al.*, *J. Magn. Magn. Mater.* **54-57**, 333 (1986).

⁵H. Takahashi and T. Kasuya, *J. Phys. C* **18**, 2697, 2709, 2721, 2731, 2745 and 2755 (1985).

⁶B. C. Sales, *Handbook on the Physics and Chemistry of Rare Earths Vol. 33* (Elsevier Science B. V., Amsterdam, 2003), p. 1.

⁷H. Harima and K. Takegahara, *J. Phys.: Condens. Matter* **15**, S2081 (2003).

⁸C. Sekine *et al.*, *Phys. Rev. Lett.* **79**, 3218 (1997).

⁹C. H. Lee *et al.* *J. Phys.: Condens. Matter* **13**, L45 (2001).

¹⁰C. H. Lee *et al.*, *J. Magn. Magn. Mater.* **272-276**, 426 (2004).

¹¹L. Hao *et al.*, *J. Magn. Magn. Mater.* **272-276** e271 (2004).

¹²H. Harima and K. Takegahara, *Physica B* **312-313**, 843 (2002).

¹³C. Sekine *et al.*, *Physica B* 281& **282**, 303 (2000).

¹⁴S. R. Saha *et al.*, *J. Phys.: Condens. Matter* **15**, S2163 (2003).

¹⁵K. Takegahara *et al.*, *J. Phys. Soc. Jpn.* **70**, 1190 (2001); **70**, 3468 (2001); **71**, 372 (2002).

¹⁶The analytical form of CF eigenenergies for T_h symmetry (Ref. 15) does not reproduce the peak at 22.7 meV observed below 20 K. The discrepancy may be explained by a coupling between the CF states and optical phonons distorting the CF potential, as the bound state in CeAl_2 studied by P. Thalmeier and P. Fulde, *Phys. Rev. Lett.* **49**, 1588 (1982). We expect a high density of states of optical phonons near the Γ_{23} level at Pr2 of $\text{PrRu}_4\text{P}_{12}$, which couple to the excitation from $\Gamma_4^{(2)}$ to Γ_{23} . However, the coupling has no direct influence on the thermal evolution of the CF schemes and should be ignored here.

¹⁷H. Harima, *Prog. Theor. Phys. Suppl.* **138**, 117 (2000).